Journal of the Geological Survey of Brazil

Zircon U-Pb SHRIMP ages of the Demêni-Mocidade Domain, Roraima, southern Guiana Shield, Brazil: extension of the Uatumã Silicic Large Igneous Province

Nelson Joaquim Reis[1], Umberto Cordani[2], Luis Emanoel Alexandre Goulart[3], Marcelo Esteves Almeida[4], Vanessa Oliveira[1], Victor Câmara Maurer[5], Ingo Wahnfried[6]

[1]CPRM - Serviço Geológico do Brasil, DIBASE/DEGEO. Av. André Araújo 2010, Manaus, Amazonas, Brazil, CEP:69.067-375
[2]USP - Universidade de São Paulo. Instituto de Geociências. Rua do Lago, 562, Butantã, São Paulo – SP, Brazil, CEP:05508-080
[3]CPRM - Serviço Geológico do Brasil. Avenida Brasil, 1731, Funcionários, Belo Horizonte - MG – Brazil, CEP: 30140-002
[4]CPRM. Serviço Geológico do Brasil – CPRM; Departamento de Recursos Minerais. Avenida Pasteur, 404, Urca, Rio de Janeiro - RJ, Brazil, CEP: 22290-255.
[5]UFOP - Universidade Federal de Ouro Preto, Departamento de Geologia. Campus Morro do Cruzeiro s/n – Bauxita, Ouro Preto – MG, Brazil, CEP: 35400-000.
[6]UFAM - Universidade Federal do Amazonas – Av. General Rodrigo Octávio Jordão Ramos, 6200, Coroado, Manaus-AM, Brazil, CEP: 69080-900.

Abstract

The Demêni-Mocidade domain (DMD) comprises a large area of granitoid rocks, located on the border between the states of Roraima and Amazonas, Brazil, within the inner part of the Ventuari-Tapajós Province of the Amazonian Craton, where large amounts of granitoid rocks, formed between 2.0-1.8 Ga, are predominant. This study examines six granite samples collected from the Mocidade and Demêni mountains, which are related in time to the Uatumã Silicic Large Igneous Province (SLIP), which, in turn, covers several tectonostratigraphic domains whose evolution is associated with an intracontinental setting, allowing a common association with I- and A-type granitoid rocks formed within the same 1.88 to 1.87 Ga time interval. These rocks are monzogranites and correspond petrographically to holocrystalline anisotropic lithotypes with fine to medium grain sizes. Their textural relationships, including some lithotypes containing phenocrysts with oscillatory zoning and resorbed rims, indicate that crystallization occurred at subvolcanic or hypabyssal depths. Moreover, the association between plutonic and subvolcanic rocks in the same suite shows variations in the crustal development of the magmatic chambers. The granitoids of the DMD share a common geochemical signature with those of the Água Branca Suite, which occurs within the Uatumã and Trombetas-Erepecuru domains of the Guiana Shield, suggesting that their crystallization occurred in similar magmatic chambers. Six U-Pb zircon ages show that most zircon crystals are concordant and the few ones which are discordant are well aligned along Discordia straight lines descending to zero. The calculated Concordia ages, covering the 1884 to 1877 Ma interval, agree within experimental error, indicating a probably similar crystallization age. Such apparent age values, close to 1900 Ma for the DMD, made it possible for the domain of the Uatumã SLIP to spread to the West, and the area of the Ventuari-Tapajós Province could extend towards the Amazonas State of Venezuela. Finally, the coexistence between I- and A-type granitoids in the DMD, with ages within the range 1.88-1.87 Ga, stimulates a discussion, and there are three possibilities: (1) The calc-alkaline magmatism can be associated with late (post-collisional) processes related to subduction. (2) The granitoid rocks are formed in an intracontinental setting under more stable (post-orogenic) tectonic conditions. (3) The granitoid rocks are predominantly formed by A-type and alkaline magmatism in intraplate settings.

Article Information

Publication type: Research papers
Received 22 Setember 2020
Accepted 19 April 2021
Online pub. 28 April 2021
Editor: E.L. Klein

Keywords:
U-Pb Geochronology;
Guiana Shield;
Roraima;
Uatumã SLIP

*Corresponding author
Nelson J. Reis
E-mail address: nelson.reis@cprm.gov.br

1. Introduction

The Ventuari-Tapajós Province is one of the five Proterozoic tectonic provinces of the Amazonian Craton (Cordani and Teixeira 2007; Figure 1A). Granitoid and volcanic rocks formed between 2.0-1.8 Ga predominate and are present in the Guiana and Central Brazil Shields.

Rock samples were collected from the Mocidade Mountain during a field survey conducted by the senior author (initial NR) and we also used samples from previous projects (Pinheiro et al. 1981) (initials EC and VC). As a consequence, a better knowledge was acquired about the geology of a little-known Amazon area, from petrographic, geochemical and geochronological studies. The Demêni-Mocidade Domain

ISSN: 2595-1939
https://doi.org/10.29396/jgsb.2021.v4.n1.4
Open access at jgsb.cprm.gov.br

was considered to be comparable with the Uatumã SLIP (Figure 1B), which occupies a vast area of the Amazonian Craton. It is covered by the Phanerozoic sedimentary covers of the Amazon basin and the Northern Pantanal depression in Roraima. In the Guiana Shield, it occurs in the south-southeast quadrant of Roraima and northeast of Amazonas State, in a varied arrangement of lineaments with NW-SE, NE-SW, and secondary E-W directions.

The tectonic significance of the Uatumã volcano-plutonism is still unclear mainly because of its large area, which makes data integration more difficult. It comprises acid plutonic rocks with high-K calc-alkaline and also alkaline affiliations, with ages ranging from 1.88 to 1.87 Ga, which are described in several other tectonostratigraphic domains of the Guiana Shield, such as the Anauá and Uatumã Domain (Figure 1C). According to Klein et al. (2012), it evolved in a post-collisional to post-orogenic intracontinental setting, allowing a common association of rocks with A- and I-type rocks with the same time interval. The spatial relationship of the Uatumã SLIP with areas with magmatic arcs in the interval from 2.04 to 1.96 Ga is considered to favor the generation of crustal sources in extensional settings (Fraga et al. 2017), and the volcano-plutonism related to an intraplate setting is consensus among many authors (Vasquez et al. 2019 and references therein). However, ages between 1.89 and 1.88 Ga obtained from lithotypes with calc-alkaline affinities have been associated with the generation of magmatic arcs (Santos et al. 2004).

The analytical data obtained in this study are helping in the development of a new interpretation of the tectonic arrangement and distribution for the northern part of the Ventuari-Tapajós tectonic province, in the Guiana Shield.

2. Geology of the Demêni-Mocidade and Uatumã domains

The Demêni-Mocidade Domain - DMD (Figure 1B, capital letter E, and Figure 1C) is one region of the Guiana Shield that is poorly studied because it is difficult to access, owing to dense forest cover, sharp mountainous relief, and table-top mountains (*tepuy*); in addition, access is restricted because it is almost entirely located in the Yanomâmi indigenous land. It includes a bordering area between the Roraima and Amazonas states that covers the low course of the Jauaperi and Alalaú rivers and the headwaters of the Demêni river in Amazonas State. In Roraima, it covers the middle course of the Catrimâni River, and the Pacu and Pauxiana tributaries. High mountainous features are seen in the Mocidade, Demêni, Corrupira, Aracá and Urucuzeiro mountain ranges, and the latter one is located on the border between Brazil and Venezuela. To the south, an extensive area with Pleistocene-Holocene sedimentary cover is formed by mega fans and dune fields (Rossetti et al. 2016 and references therein).

The DMD comprises a large area of granitoid and orthogneiss rocks, which were hierarchically classified as a group, suite, or complex (e.g., Moura, Urariquera, Rio Urubu, Cauaburi), as a general rule, forming the basement for some geomorphological features, such as table mountains *(tepuys*), e.g., the Aracá Table. In the bordering area between Brazil and Venezuela, in the Imeri-São Carlos Domain (Figure 1B), similar rocks were included in the São Carlos Metamorphic-Plutonic Association (Wynn et al. 1994), and Rb-Sr whole-rock and U-Pb ages were obtained by Gaudette and Olszewski (1985) within the range 1.86-1.76 Ga. Geological integration with the neighboring domains has not yet been established.

Within the DMD, two main structural linear patterns interact: a) a system formed by NE-SW shear-zones linked to a mid-Proterozoic 1.33 -1.30 Ga K'Mudku tectonic episode (Santos et al. 2006, Cordani et al. 2010), cutting through a Paleoproterozoic basement formed in two main time intervals (Rio Urubu Belt, 1.94-1.92 Ga, and Imeri-São Carlos Domain, 1.83-1.76 Ga - Figure 1B), and b) a system characterized by NW-SE shearing zones with 1.52-1.48 Ga (Almeida et al. 2013), associated with the Uatumã SLIP (1.88-1.87 Ga). Mylonites and ultramylonites are produced by brittle-ductile events, with physical conditions typical of the greenschist facies.

The sedimentary rocks of the Aracá Table, in the Corrupira mountain range (Figure 1 C), are considered to cover a basement dated by Santos (2003) at 1798 Ma. This author, measuring detrital zircon grains, indicated ages associated with the Uatumã SLIP and with the Rio Urubu Belt, as well as older Paleoproterozoic ages of 2.04-2.01 Ga, which could be related to the Trairão and Anauá regions (Figure 1B).

The Uatumã Domain (UD – after Reis et al. 2006) is located in the south-southeast portion of Roraima State and the northeast part of Amazonas State (Figure 1B, capital letter A and C, and Figure 1C). In this region, the effusive and pyroclastic rocks were first included in the Iricoumé Group and associated with granitoids of the Mapuera Suite, belonging to the Uatumã Supergroup (Costi et al. 1984). In this area, Oliveira et al. (1996) identified calc-alkaline granitoids, correlated them with the Água Branca Suite, and attributed a magmatic arc environment to them. Macambira et al. (2002) found an age of 1.89 Ga (Table 1) for the volcanic group of the Jatapu River hydroelectric plant. These authors maintained the name "Iricoumé" for these rocks, but observed its association with the Água Branca granitoids, interpreted as formed in a post-collisional setting (Almeida and Macambira 2007).

The calc-alkaline volcanic-plutonic of this sector of Roraima was nominated "Jatapu" (Fraga and Reis 2002, Reis et al. 2004), as it was believed to be distinct from the one located in the northern portion of the State. In this work, the volcanic component is designated as "Rio Jatapu Group". Santos et al. (2011) detected a charnockitic magmatism with 1.87 Ga and integrated it into the Uatumã event (Table 1). The volcano-plutonism extends to the south of Guyana (Figure 1B, capital letter B), where it is linked to the Kuyuwini Group, which comprises volcanic rocks associated with granitoid plutons, such as Kamoa, Amuku, Maopytian, Onoro and Yukanopito (Berrangé 1977).

On the border between Roraima and Amazonas (Figure 1B, capital letter C), along the BR-174 highway, which connects Manaus to Boa Vista, U-Pb SHRIMP ages ranging from 1.88 to1.87 Ga were determined for metagranitoids and orthogneisses (Santos et al. 2002), which were later included in the Jauaperi Complex (Reis et al. 2006). In the area of the Pitinga mine and surroundings, similar ages were determined for the Iricoumé-Mapuera volcano-plutonic association, showing alkaline and A-type affinities (Costi et al. 2009, Ferron et al. 2010, Marques et al. 2014), while Pb-Pb evaporation ages of 1.89 Ga were related to I-type calc-alkaline granitoids, associated with the Água Branca Suite (Almeida and Macambira 2007, Valério et al. 2012).

In the northwest of the Pará State (Figure 1B, capital letter D), Barreto et al. (2013) described ignimbrite with Pb-

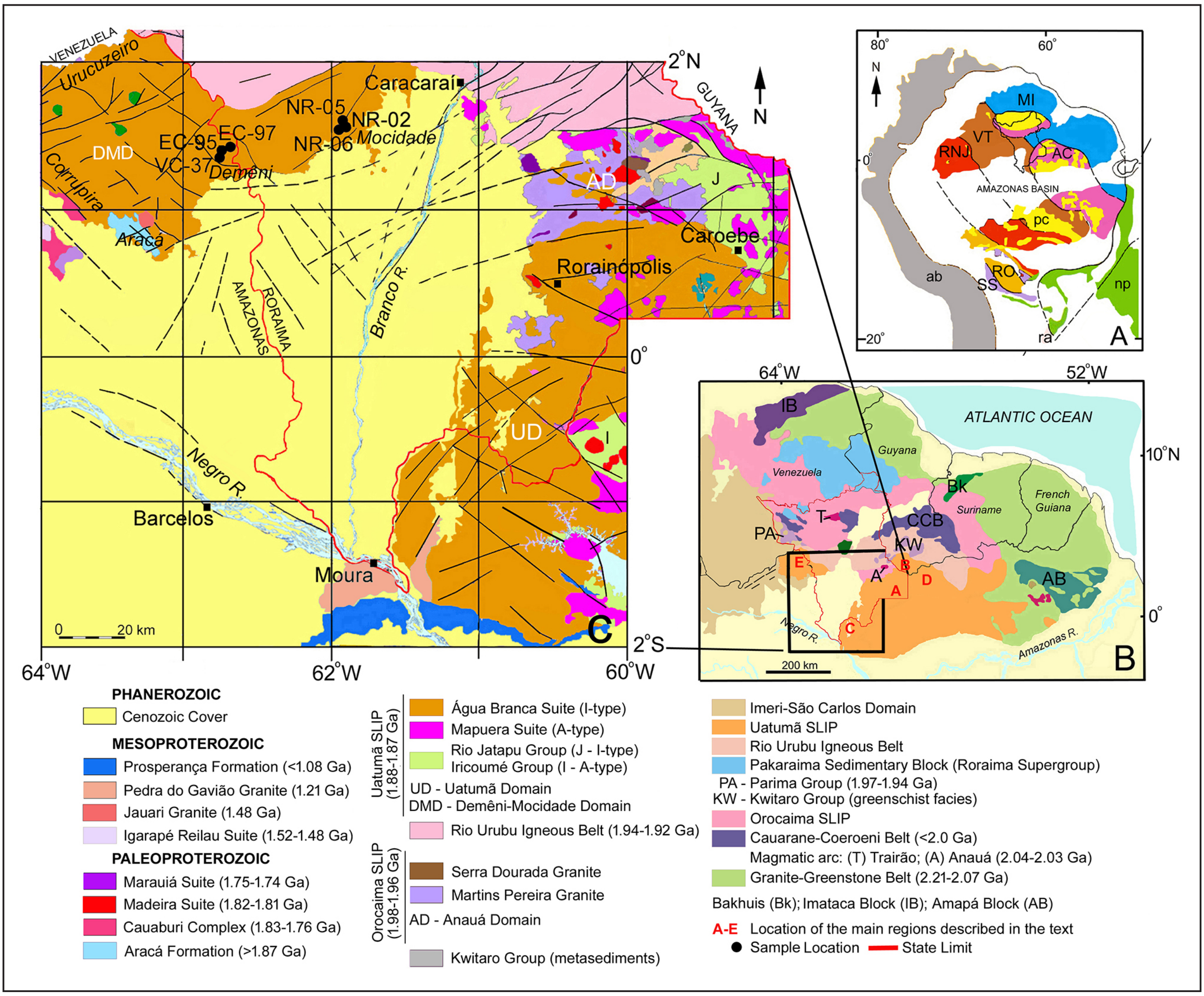

FIGURE 1. Amazonian Craton and their geochronological provinces (Cordani and Teixeira 2007): AC – Amazônia Central (>2.6 Ga); MI – Maroní-Itacaiúnas (2.25-2.05 Ga); VT – Ventuari-Tapajós (2.00-1.80 Ga); RNJ – Rio Negro-Juruena (1.78-1.55 Ga); RO – Rondoniano-San Ignácio (1.50-1.30 Ga); SS – Sunsás-Aguapeí (1.25-1.00 Ga); ra – Rio Apa Block; np – Neoproterozoic tectonic provinces; ab – Andean belt; pc – Phanerozoic cover. B – Simplified geological map of the Guiana Shield (after Fraga et al. 2017); C – Geological sketch of the Demêni-Mocidade (DMD), Anauá (AD) and Uatumã (UD) domains (adapted from Reis et al. 2004).

Pb evaporation ages of 1.88 Ga, and associated them with the Iricoumé Group. Moreover, Leal et al. (2018), for the same region, determined U-Pb zircon ages for granitoids of the Mapuera and Água Branca suites (Table 1).

3. Geophysical framework of the study area

The geological framework of the area of the Demêni, Aracá and Catrimâni rivers was evaluated in recent years using geophysical-geological interpretation maps (Oliveira 2018, Rocha et al. 2018, Chiarini et al. 2018) integrated with a few results from regional remote surveys.

Figure 2 (Correa 2019) shows the magnetic and gravimetric signatures for the area of geophysical surveys done for the Demêni-Mocidade and Uatumã Domains in the Roraima-Amazonas boundary region. The magnetic anomaly data were filtered to the 15 km upward continuation in order to enhance the crustal influence and reduce the importance of anomalies from shallow sources.

A low to intermediate magnetic signature is indicated with green and blue colours (Figure 2A) for the Demêni-Mocidade Domain, where the NE-SW trending lineaments were related by Almeida et al. (2013) to the younger tectonic events of 1.33-1.30 Ga age. The NE-SW tectonic trend is also predominant in the Uatumã Domain; however, it is interrupted by a large areal strip, with a magnetic high feature showing a roughly N-S trend, occupying the region along the Branco River. In addition, NW-SE trending lineaments associated with magnetic highs, where the rocks yielded ages in the 1.52-1.48 Ga interval (Almeida et al. 2013), are also important within the Demêni-Mocidade Domain. They control the sedimentary plateau of the Aracá Table, and their NW-SE trends seems to be derived from a dextral cinematics.

The gravity pattern (Figure 2B), at its eastern and western sides, indicates intermediate values in green and orange colours. However, it shows NE-SW and N-S trending gravimetric highs (red colours) cutting through the previous features.

4. Analytical methods

4.1. U-Pb zircon geochronology

Six rock samples from Demêni and Mocidade Mountains were dated by U-Pb geochronology (Figure 1C) at the Geochronology Research Center (CPGeo) of the University of São Paulo (USP) using a SHRIMP-IIe/MC instrument. Details of analytical procedures, including calibration methods, were presented by Williams (1998) and Sato et al*.* (2014). Initially, zircon grains from samples were separated using standard procedures, such as heavy-liquid separation and a Frantz magnetic separator.

Selected zircons, together with some fragments of the Temora-2 reference zircon (417 Ma; Black et al. 2003), were mounted into epoxy resin discs with a diameter of 2.54 cm, and polished with diamond compound (1 – 7 μm) to expose grain cores. The mount was covered with a gold layer for zircon imaging and dating. Cathodoluminescence (CL) images of mounted and polished grains were obtained by means of a FEI Quanta 250 Scanning Electron Microscope (SEM) and XMAX CL detector (Oxford Instruments). For details of the analytical procedures, see Sato et al. (2014). Zircon CL images were used to interpret the internal structure of crystals and to select the best areas for isotopic analysis. In the analytical procedures, U concentration and 206Pb/238U ratio were calibrated using Sri Lanka SL13 (U = 238 ppm, Williams 1998) and Temora-2 zircon standard, respectively.

Individual ages were determined on the basis of five successive scans of the mass spectrum, and the average ages reported in the study were weighted mean $^{207}Pb/^{206}Pb$ ages with confidence limits of 95%. The correction for common Pb was made using the measured ^{204}Pb value, and the typical error for the $^{206}Pb/^{238}U$ ratios is less than 2 percent. The data, presented at 1 sigma level, were reduced using the SQUID software. Moreover, the Concordia diagrams and the probability density plots were prepared by means of Isoplot / Excel (Ludwig 2009a, b).

4.2. Lithogeochemistry

Whole-rock chemical analyses were performed at the SGS Geosol Laboratories Ltda., Vespasiano, MG, Brazil. After cleaning, samples were crushed and sieved to grain sizes < 120#.

To measure major element oxides, a glass bead was produced by Li-tetraborate fusion and analyzed by XRF. In the case of trace elements, Li-metaborate flux was used for sample digestion, and concentrations were determined by ICP-OES/ICP-MS. Rare earth elements were quantified using multi-acid digestion of samples and measured by ICP-OES/ICP-MS. LOI (loss on ignition) was obtained by sample calcination at 405º/1000ºC. The results of the geochemical analyses and the diagrams prepared for this paper were generated using IGPET 05 software.

5. Results

5.1. Petrography

Nine samples from the Demêni and Mocidade mountains were observed under a conventional optical microscope, and they were classified as monzogranites, with subordinate mylonitic rocks or rocks with garnet. Table 2 and Figure 3 show the modal composition and classification, respectively.

The rocks contain biotite as the main mafic mineral and, occasionally, clinopyroxene, in addition to Fe-Ti oxides. Allanite is the most common accessory mineral, followed by apatite, monazite, epidote s.s., and zircon. In the most altered rocks, sericite, epidote and carbonate replace phenocrysts of plagioclase and K-feldspar, and primary biotite is replaced with chlorite. Secondary biotite flakes are formed from clinopyroxene (EC-5 sample), as well as within K-feldspar fractures, especially in mylonitic rocks.

NR-02, NR-05, NR-06 (two thin-sections), NR-08, NR-09D, EC-95 and VC-037 samples correspond petrographically to holocrystalline anisotropic lithotypes with fine to medium grain sizes. Their texture is hiatal (Figures 4A and B), characterized by euhedral to subhedral phenocrysts of plagioclase and K-feldspar ranging from 3 to 5 mm, commonly with oscillatory zoning and rims with albite overgrowth, immersed in a fine matrix composed of K-feldspar, quartz, plagioclase and subordinate biotite. Plagioclase phenocrysts, with or without oscillatory zoning, usually show resorption/reprecipitation rims, indicating complex crystallization processes during magma rise. Crystal twinning is rare. Perthitic phenocrysts with albite exsolution lamellae are common, as well as micrographic or granophyric texture in crystalline rims.

In the matrix, crystals of intergranular anhedral microcline hosting quartz crystals are common. The above-mentioned textural relationships are usually associated with rocks crystallized in subvolcanic or hypabyssal depths.

In the NR-08 thin section (Figure 4C), both glomerophiric and hiatal porphyritic textures are characterized by euhedral to subhedral garnet xenocrysts and subordinate euhedral to anhedral allanite grains. The anomalous extinction of some garnet grains suggests a strong contribution of the calcium or aluminum component (spessartine or grossular).

The NR-09D thin section shows coarse to medium grain size and inequigranular porphyritic hypidiomorphic to equigranular texture, which are less representative of the collection described above. The textural relationships of the rocks indicate a crystallization in a plutonic environment. NR-09D and EC-97 samples correspond to deformed rocks and, in general, show hypidiomorphic porphyritic (EC-97) or hiatal (NR-09D) textures, which were affected by the development of mylonitic foliations (Figure 4D). The NR-09D sample, in particular, shows shear band, where the inequigranular hiatal porphyritic texture was obliterated by the development of a low-temperature mylonitic foliation, marked by the oriented recrystallization of biotite, K-feldspar, quartz, and plagioclase, followed by cataclasis. In general, cataclasites show porphyroclasts with pressure shadow, formed by feldspar or, less commonly, allanite.

Comparatively, samples of the Demêni-Mocidade Domain show similarities with the biotite granite facies described for the Água Branca Suite (Almeida and Macambira 2007), which comprises, in its type-area, monzogranites, granodiorites and, more rarely, syenogranites with enclaves of biotite-hornblende tonalites.

5.2. Geochemistry

The geochemical results for the rocks of the Demêni-Mocidade Domain covered by this study are shown in

TABLE 1. Summary of geochronological data for the Uatumã SLIP in the Guiana Shield. Methods: E: $^{207}Pb/^{206}Pb$ evaporation; S: U/Pb SHRIMP; L: U/Pb LA-ICP-MS. bt – biotite; hb – hornblende; kf - alkali feldspar.

Stratigraphic Units	Rock Type	Age (Ma)	Method	References
SE RORAIMA				
Água Branca Suite	quartz-monzodiorite	1895 ± 3	E	Almeida (2006)
Água Branca Suite (Caroebe)	biotite granodiorite	1891 ± 2	E	Almeida (2006)
Água Branca Suite (Caroebe)	granitoid	1898 ± 2	E	Almeida (2006)
Água Branca Suite	hb-bt monzogranite	1901 ± 5	E	Almeida (2006)
Água Branca Suite (Ig. Azul)	granitoid	1891 ± 6	E	Almeida (2006)
Água Branca Suite (Ig. Azul)	granitoid	1889 ± 2	E	Almeida (2006)
Rio Jatapu Group	andesite	1893 ± 5	E	Almeida (2006)
Santa Maria Enderbite	enderbite	1891 ± 1	E	Almeida (2006)
Murauaú Granite	granite	1871 ± 5	E	Almeida (2006)
Rio Jatapu Group	dacite	1893 ± 2	E	Macambira et al. (2002)
Água Branca Suite	biotite granite	1882.6 ± 9	S	This study (NR-02)
Água Branca Suite	biotite granite	1878 ± 12	S	This study (NR-05)
Água Branca Suite	biotite granite	1884.4 ± 8	S	This study (NR-05)
Água Branca Suite	biotite granodiorite	1878.5 ± 6,9	S	This study (VC-37)
Água Branca Suite	biotite granodiorite	1880.5 ± 7	S	This study (EC-95)
Água Branca Suite	biotite granite	1877.7 ± 4,9	S	This study (EC-97)
Mapuera Suite	(meta)granite	1868 ± 8	S	Santos et al. (2002)
Mapuera Suite	(meta)granite	1867 ± 15	S	Santos et al. (2002)
Mapuera Suite	granitoid	1879 ± 3	S	Santos et al. (2002)
Mapuera Suite	granitoid	1880 ± 3	S	Santos et al. (2002)
NE AMAZONAS				
Iricoumé Group	rhyolite	1882 ± 2	E	Ferron et al. (2010)
Iricoumé Group	rhyolite	1885 ± 8	E	Ferron et al. (2010)
Iricoumé Group	rhyolite	1881 ± 2	E	Ferron et al. (2010)
Iricoumé Group	rhyolite	1886 ± 6	E	Ferron et al. (2010)
Iricoumé Group	andesite	1892 ± 2	E	Ferron et al. (2010)
Iricoumé Group	ignimbrite	1890 ± 2	E	Ferron et al. (2010)
Iricoumé Group	andesite	1897 ± 2	E	Ferron et al. (2010)
Mapuera Suite	biotite monzogranite	1888 ± 3	E	Ferron et al. (2010)
Mapuera Suite	biotite monzogranite	1885 ± 3	E	Ferron et al. (2010)
Mapuera Suite	sienogranite	1882 ± 3	E	Ferron et al. (2010)
Mapuera Suite	biotite granite	1882 ± 4	E	Ferron et al. (2010)
Mapuera Suite	bt-kf granite	1885 ± 4	E	Ferron et al. (2010)
Mapuera Suite	sienogranite	1882 ± 2	E	Ferron et al. (2010)
Mapuera Suite	biotite sienogranite	1875 ± 4	E	Ferron et al. (2010)
Mapuera Suite	biotite granite	1889 ± 2	E	Valério (2006)
Iricoumé Group	rhyolite	1883 ± 4	E	Valério (2006)
Iricoumé Group	ignimbrite	1896 ± 7	E	Valério (2006)
Iricoumé Group	riodacite	1896 ± 7	S	Santos et al. (2002)
Iricoumé Group	rhyolite	1888 ± 3	E	Costi et al. (2000)
Mapuera Suite	granite	1861 ± 20	S	Lenharo (1998)
Mapuera Suite	granite	1864 ± 13	S	Lenharo (1998)
Mapuera Suite	granite	1865 ± 15	S	Santos (2003)
Mapuera Suite	granite	1871 ± 5		Almeida (2006)
Mapuera Suite	hastingsite granite	1871 ± 5	S	Santos et al. (2002)
Jaburu Charnockite	charnockite	1873 ± 6	S	Santos et al. (2001)
Mapuera Suite	granitoid	1876 ± 4	S	Santos et al. (2002)
Água Branca Suite	biotite granite	1890 ± 2	E	Valério (2006)
Água Branca Suite	biotite granite	1895 ± 6	E	Valério (2006)
Água Branca Suite	bt-hb granite	1893 ± 3	E	Valério (2006)
Iricoumé Group	rhyolite	1869 ± 12	E	Lenharo (1998)
Iricoumé Group	rhyolite	1882 ± 11	L	Marques et al. (2014)
NW PARÁ				
Iricoumé Group	ignimbrite	1888 ± 2.5	E	Barreto et al. (2013)
Iricoumé Group	ignimbrite	1889 ± 2	E	Barreto et al. (2013)
Água Branca Suite	granitoid	1887.5 ± 4.8	L	Leal et al. (2018)
Mapuera Suite	granitoid	1881 ± 8.1	L	Leal et al. (2018)
Água Branca Suite	monzogranite	1886 ± 4,8	L	Viana et al. (2016)
Mapuera Suite	bt-kf granite	1870 ± 14	L	Viana et al. (2016)

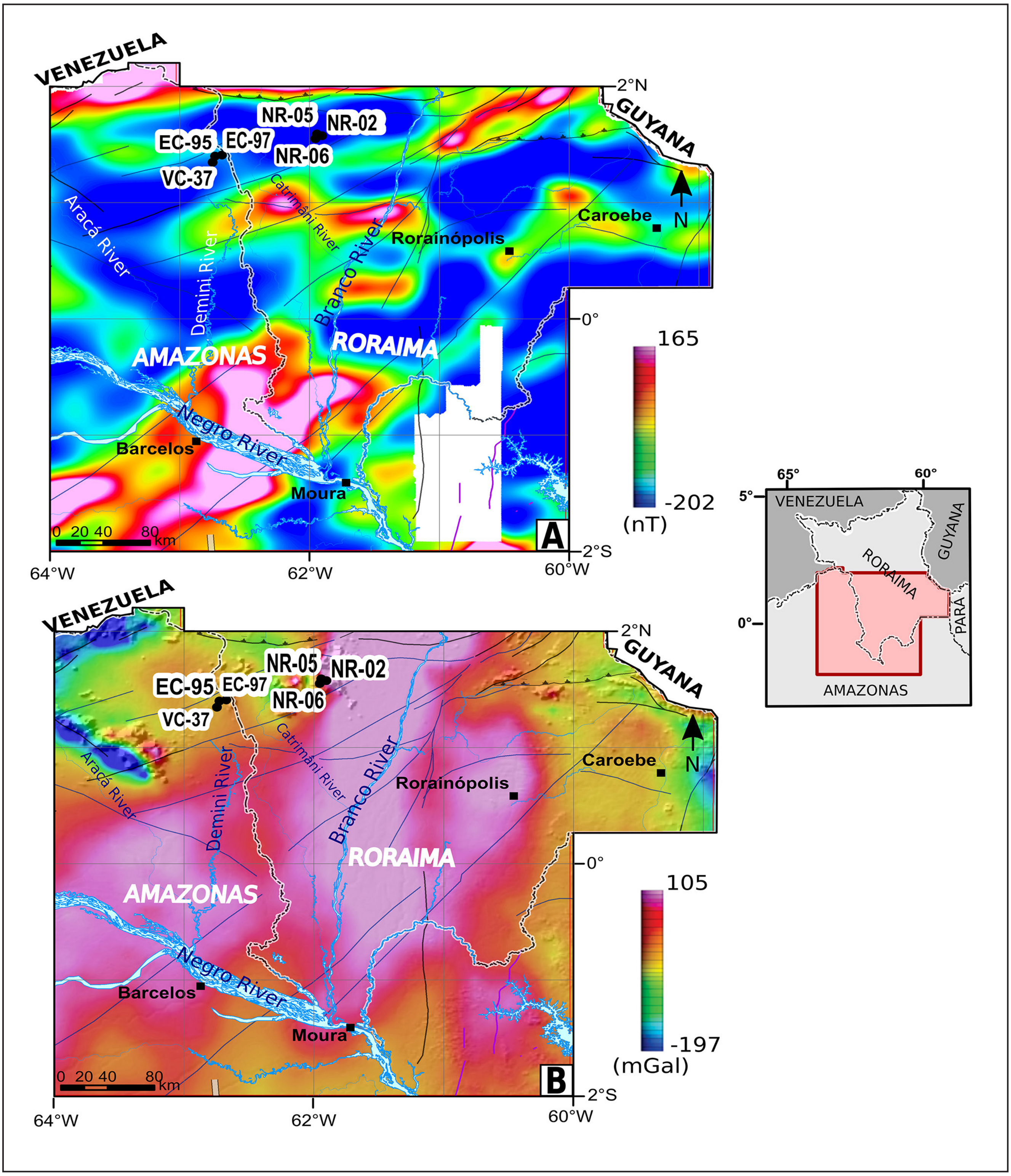

FIGURE 2. A – Anomalous magnetic field pattern (nT) from Correa (2019); B – Bouguer anomaly pattern (mGal) on the Digital Terrain Model – DTM.

Table 3. In the diagrams of Figure 5, they have a chemical behavior similar to that of the Água Branca Suite (Almeida and Macambira 2007).

The K_2O contents of lithotypes are in the range 4.60-5.73% and define high-K calc-alkaline granitoids in the limit with the shoshonitic field (Figure 5A). The Na_2O+K_2O-CaO index values (modified alkali-calcic index diagram – MALI, Frost et al. 2001) show a well-defined calc-alkaline composition of these rocks (Figure 5B) in which the A/CNK (aluminum saturation index ≈ 0,71 -1,11) and A/NK (≈1,18-2,20) ratios point to a metaluminous to slightly peraluminous character (Figure 5C). The molar proportions of the rocks of the Água Branca Suite define a more expanded range, indicating a slightly more peraluminous signature in some lithotypes.

The granitoids of the Demêni-Mocidade Domain, compared to the average composition of the rocks of the Água Branca Suite, show a higher degree of oxidation, defined by the geochemical values of the Fe number (Fe# or Fe_2O_3t /

TABLE 2. Modal composition, nomenclature and textural aspects of the rock types analyzed in this study. A.M. altered minerals: sericite, epidote, chlorite, carbonate and biotite.

Sample	EC-95	VC-37	NR-02	NR-05	NR-06L1	NR-06L2	NR-09D	NR-09	EC-97	NR-08
Location	Demêni		Mocidade						Demêni	Mocidade
Rock	Monzogranite							Mylonitic Monzogranite		Garnet-bearing Monzogranite
Texture	Inequigranular porphyritic to hiatal						porphyritic	Mylonitic and cataclastic, subordinately with relic eu-hedral to subhedral, hiatal, and porphyroclastic		Hiatal and glomerophyric
Modal Composition										
Kfs	28	30	32	30	30	35	40	37	35	35
Pl	45	43	39	45	43	40	37	34	37	25
Qtz	19	20	24	18	20	20	20	20	18	18
Bt	5	7	5	7	7	5	3	7	10	1
Cpx	2	-	-	-	-	-	-	-	-	-
Fe-Ti oxide	-	-	-	-	1	< 1	< 1	< 1	< 1	< 1
Aln	1	< 1	-	-	0	< 1	< 1	2	< 1	1
Ep	< 1	< 1	< 1	-	1	-	-	< 1	< 1	3
Grt	-	-	-	-	-	-	-	-	-	17
Ttn	< 1	< 1	-	<1	1	< 1	-	< 1	< 1	< 1
Ap	< 1	< 1	< 1	< 1	1	-	< 1	< 1	< 1	< 1
Mnz	< 1	< 1	< 1	< 1	1	< 1	<1	< 1	< 1	< 1
Zrn	< 1	< 1	< 1	< 1	1	< 1	<1	< 1	< 1	< 1
A.M.1	< 1	< 1	< 1	< 1	< 1	< 1	< 1	< 1	< 1	< 1

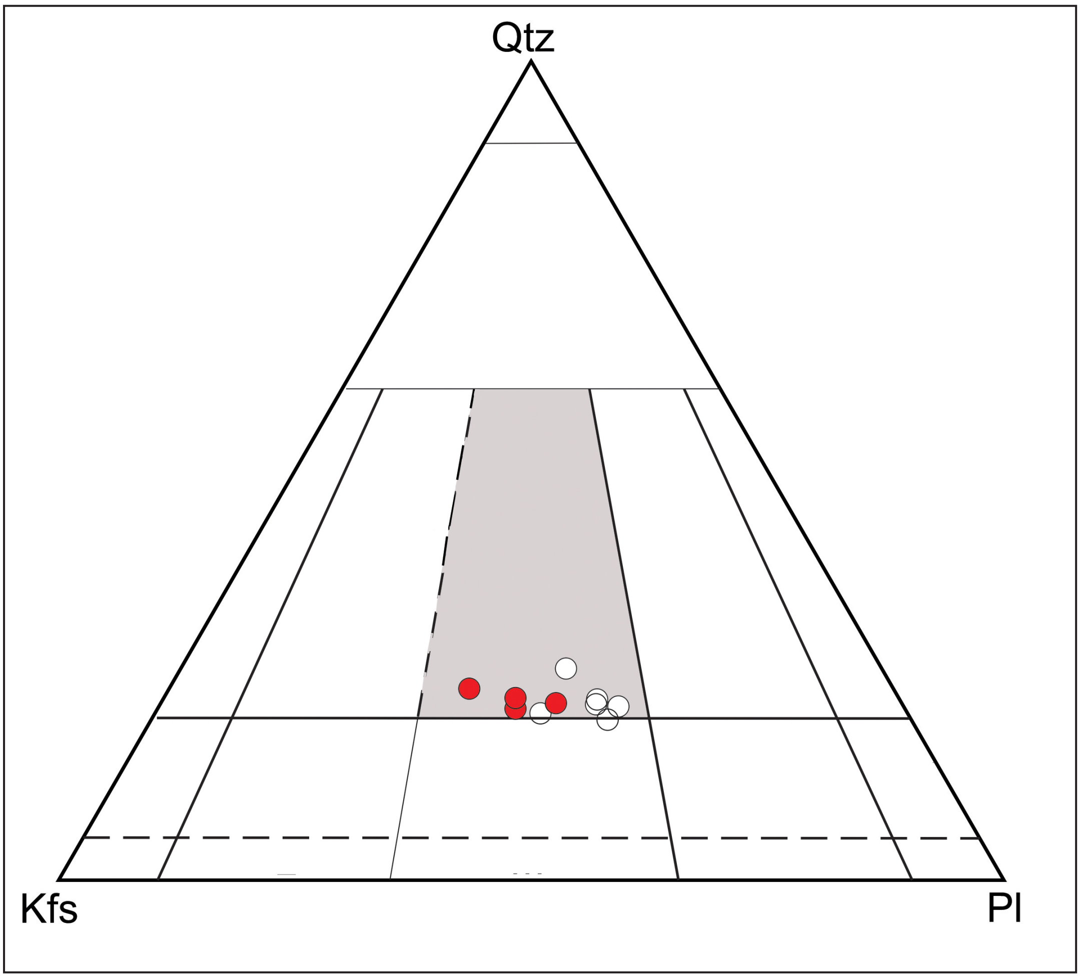

FIGURE 3. Modal QAP diagram (Streckeisen 1976) for the Demêni (red circles) and Mocidade (empty circles) granitoids. The grayish area corresponds to monzogranites. Qtz - quartz, Kfs - alkali feldspar, Pl - plagioclase.

(Fe_2O_3t + MgO). In the Fe# versus SiO_2 diagram (Figure 5D), the mentioned lithotypes are discriminated by the highest Fe# values, showing that the Água Branca rocks are predominantly magnesian, while the Demêni-Mocidade granitoids are predominantly ferroan, but with a composition close to the limit of the magnesian field.

Analytical results for the granitoids show enrichment in Zr (≈ 142-382 ppm), Y (≈ 19-43 ppm) and light rare earth elements – LREE (e.g., Ce ≈ 83-142 ppm) comparable to that of the Água Branca Suite. Multi-element geochemical patterns are characterized by large ion lithophile element - LILE enrichment (Ba, Rb, Cs, K), high field strength element - HFSE (Th and U) and REE (especially, the light ones) that highlight and define pronounced negative anomalies of Ti (TiO_2 ≈ 0.34-1.01%) and Nb (≈ 13.6-22.3 ppm) (Figure 5E).

A common signature is also shown in the REE diagrams normalized to C1 chondrite (Sun and McDonough 1989). The granitoids have a linear to poorly depleted pattern of heavy rare earth elements – HREE with [Gd]/[Yb]n ratios ≈ 1.22-2.29 and are enriched 15 to 40 times the chondritic values. The enrichment in LREE is marked by values of [La]n varying from 100 to 300 times the chondritic values, and the relative depletion in HREE is marked by [La]/[Yb]n ≈ 8.46-28.78 and [Gd]/[Yb]n ≈ 1.22-2.29. The ETR patterns also point to negative Eu anomalies (Eu/Eu * ≈ 0.61-0.79 (Figure 5F).

5.3. U-Pb zircon geochronology

U-Pb SHRIMP dating was performed for zircons from six granitoids of the Mocidade (NR-02, NR-05 and NR-06) and Demêni Mountain (VC-37, EC-95 and EC-97), and their location is shown in Figure 1C. These are the UTM coordinates of the six samples analyzed in this study: NR-02 (623049/176616); NR-05 (621502/177714); NR-06 (621354/176979); VC-37 (500288/160376); EC-95 (506795/161845) and EC-97 (519179/169049). The geochronological results of the U-Pb zircon dates are shown in Table 4. CL-images and Concordia diagrams are shown in Figures 6 and 7, respectively.

5.3.1. Sample descriptions and corresponding U-Pb zircon ages

NR-02 Sample - Zircon grains of this sample are non-equidimensional, with length ranging from 100 to 250μm. The grains are commonly euhedral, elongated to short prismatic, showing well-defined oscillatory concentric and sector zoning. Occasionally, rims with structures of magmatic resorption

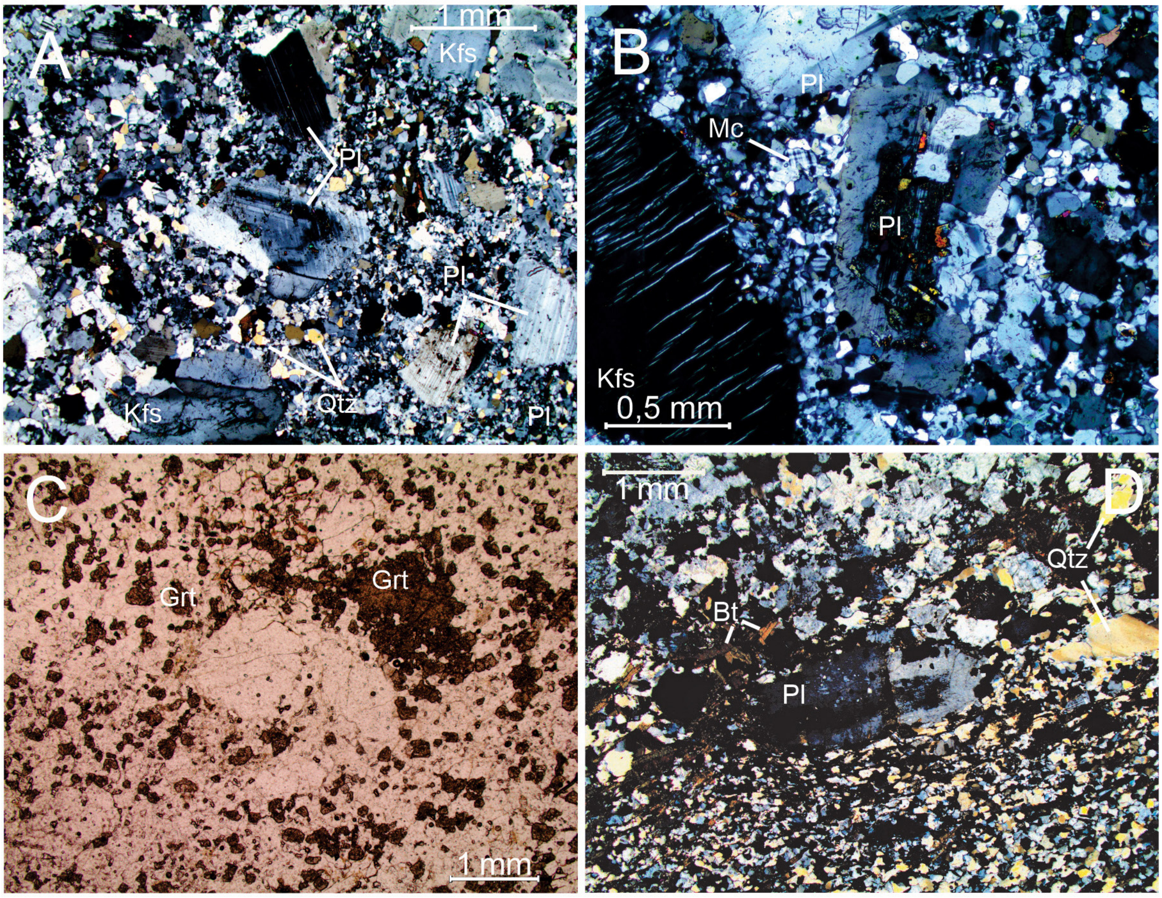

FIGURE 4. Photomicrographs. A – Inequigranular hiatal porphyritic texture. Details of the subhedral plagioclase phenocryst with oscillatory zoning (sample EC-95, crossed polarizers, 2X magnification); B – Details of EC-95 sample, with phenocrysts in an inequigranular hiatal porphyritic texture, with zoned plagioclase in the center of the photomicrograph and perthitic K-feldspar on the bottom left corner. Both crystals show slightly irregular rims, suggesting resorption processes (crossed polarizers, 4X magnification); C – Glomerophiric texture formed mainly by garnet xenocrysts. The texture coexists with the hiatal porphyritic texture (NR-08 sample, parallel polarizers, 2X magnification); D – Inequigranular hiatal relic texture affected by the development of low-temperature mylonite. In the center of the photomicrograph, porphyroclast of zoned plagioclase (NR-09 sample, crossed polarizers, 2X magnification).

TABLE 3. Whole-rock analyses of the six Demêni-Mocidade samples. *D.L.– detection limit

		EC-95	EC-97	VC-37	NR-02	NR-05	NR-06
Oxide (wt %)	SiO_2	66.0	65.3	68.3	70.8	67.9	68.1
	TiO_2	0.52	1.01	0.48	0.34	0.41	0.42
	Al_2O_3	16.4	14.7	15.9	14.6	16.0	16.0
	Fe_2O_3	3.48	5.6	3,00	2.52	3.22	3.41
	MnO	0.06	0.1	0.05	0.06	0.08	0.1
	MgO	0.86	1.14	0.73	0.54	0.66	0.74
	CaO	3.29	3,00	2.55	1.82	1.97	2.42
	Na_2O	3.6	2.98	3.7	3.69	4.11	3.78
	K_2O	4.74	5.36	4.9	5.14	4.95	4.8
	P_2O_5	0.129	0.403	0.116	0.081	0.117	0.121
	BaO	0.15	0.18	0.13	0.14	0.17	0.1
	Cr_2O_3	0.01	0.01	<0.01*	<0.01*	<0.01*	<0.01*
	Nb_2O_5	<0.05*	<0.05*	<0.05*	<0.05*	<0.05*	<0.05*
	V_2O_5	<0.01*	<0.01*	<0.01*	<0.01*	<0.01*	<0.01*
	LOI	0.16	0.32	0.52	0.54	0.91	0.59
	Total Sum	99.42	100.1	100.38	100.27	100.5	100.58
Trace Element (ppm)	Ni	7	6	7	5	6	5
	Cr	0.01	0.01	0.01	0.01	0.01	0.01
	Rb	159.7	160.9	179	146.9	174.1	187.7
	Cs	5.1	3.03	3.2	5.96	2.32	7.62
	Ba	1174	1500	1298	639	1136	1422
	Sr	493.1	415.6	428.7	252.4	447	507.7
	Ga	18.4	20.3	18.9	12.4	14.8	19.4
	Ta	0.94	0.98	0.99	0.9	0.82	1.2
	Nb	13.6	22.3	15.7	14.2	13.5	15.3
	Hf	6.68	9.56	7.72	4.47	4.43	7.32
	Zr	230.2	381.8	274.6	141.6	214.9	273.5
	Y	21.89	32.91	43.06	18.68	27.04	20.69
	Th	16.4	7	11.8	17.4	12.4	20.5
	U	4.83	2.39	2.99	4.22	3.38	5.27
REE (ppm)	La	47.6	64.3	46	43.1	58.6	31.2
	Ce	94.2	142.1	91.9	83	114.1	86.8
	Pr	10.09	15.12	10.79	8.81	13.5	8.47
	Nd	36.8	59	40.6	31.4	41.1	31.2
	Sm	6.3	10.2	7.4	5.2	7.7	5.6
	Eu	1.42	2.52	1.53	0.99	1.28	1.23
	Gd	5.3	9.13	6.67	4.39	5.27	4.48
	Tb	0.72	1.29	1	0.67	0.74	0.66
	Dy	4.04	6.6	6.08	3.51	4.37	4.12
	Ho	0.81	1.25	1.45	0.72	0.9	0.81
	Er	2.29	3.63	3.96	2.17	2.76	2.46
	Tm	0.35	0.48	0.56	0.32	0.42	0.38
	Yb	2.6	3.3	3.9	2.3	2.6	2.4
	Lu	0.39	0.48	0.59	0.35	0.36	0.37
	Eu/Eu*	0.75	0.79	0.66	0.63	0.61	0.75

indicate that some crystals were reworked by a late magmatic process (grains 4.1 and 5.1, Figure 6). The analyses yielded concentrations of U ≈ 172-412 ppm, Th ≈ 112-1259 ppm and Th/U ratios ≈ 0.66-1.40. Isotopic analysis yielded ^{207}Pb / ^{206}Pb apparent ages ranging from 1903 to 1856 Ma. In the assembly of selected grains, one single older concordant zircon (that yielded an age of 1903 Ma stands out. This analyzed grain is consistent with antecrysts described by Miller et al. (2007).

A group of eight analyses with degrees of discordance ranging from -2 to 19% defined a Pb-loss line that intercepts the Concordia curve at 1882.6 ± 9.0 (±11) Ma and finishes at the origin. In other model, six concordant analyses yielded a Concordia age of 1884.1 ± 4.5 Ma (autocrysts of Miller et al. 2007). The overlap in the errors of these two models shows that this latter result is the best approximation to the crystallization age.

NR-05 Sample - This sample is formed mostly by short-prismatic grains. Mineral inclusions are rare in selected zircons. The grains range from 100-200µm and exhibit well-defined concentric zoning. In the outer rim of the grains, a thin overgrowth with sign of magmatic resorption is occasionally observed (grains 1.1 and 6.1, Figure 6). Spot measurements for the domains showed concentrations of U = 136-1275 ppm and Th = 98 - 1081 ppm. Despite the broad range of values, Th/U ratios ≈ 0.42-1.26 suggest that mixed domains were analyzed in zircons. Zircon grains yielded ^{207}Pb/ ^{206}Pb apparent ages between 1893 and 1830 Ma, with wide overlap within error and degrees of discordance ranging from -1 to 5%. Considering the lower intercept at the origin, $^{207}Pb/^{235}U$ and $^{206}Pb/^{238}U$ isotopic ratios (8 analyses) form a coarse distribution along a Pb-loss line that intercepts the Concordia curve at 1878 ± 12 (±13) Ma. In a second model, four analyses with degrees of discordance between -1 and 2% yielded a Concordia age of 1874 ± 6.9 Ma. The overlap within the error observed between the models, combined with the lack of concordant analyses, allowed us to interpret the result of the latter model as the rock crystallization age.

NR-06 Sample - Zircons from the sample are generally prismatic euhedral to subhedral crystals, with sizes ranging from 150 to 250µm. In CL images (Figure 6), the grains show well-defined concentric zoning, although domains with poorly defined sector zoning were found in some crystals (for example, NR-06, grain 1.1). Resorption structures in external rims are common in some grains (grain 1.1). More rarely, mineral inclusions and core xenocrysts were found in some grains (NR-06, grains 6.1 and 7.1). At moderate concentrations of U (≈ 224-499 ppm) and Th (≈ 156-308), spot analyses showed Th/U ratios ranging between ≈ 0.63-0.93. With degrees of discordance ranging from -3 to -2%, zircon dating yielded $^{207}Pb/^{206}Pb$ apparent ages between ≈ 1857 and 1899 Ma. The grain (6.1) from sample NR-06 (Figure 6) yielded a concordant $^{207}Pb/^{206}Pb$ apparent age of 1899 Ma (possible antecrystal). Eight isotopic analyses of selected zircons plot along a lead-loss line and indicated the upper intercept age of 1884.4 ± 8.6 (± 10) Ma (Figure 7).

Four analyses with -2 and 2 % discordance yielded a Concordia age of 1883.9 ± 4.8 Ma, interpreted as the crystallization age of this rock and, again, the oldest zircon points to an apparent age of 1.889 ± 10 Ma.

EC-95 Sample – CL images of zircons showed predominantly subhedral crystals with grain size ranging from 80 to 150 µm. Several grains are apparently zircon fragments that were formed during resorption over a long period of magmatic activity (grains 6.1, 9.1 and 12.1, Figure 6). These processes also formed rounded grains with domains showing discontinuous concentric oscillatory zoning. SHRIMP spot analyses yielded low U (≈ 127-354 ppm) and Th (≈ 74-248) contents, resulting in Th/U ratios ranging from ≈ 0.6 to 1.0. The apparent age reflects a degree of discordance ranging between -8 and 26%. $^{207}Pb/^{206}Pb$ apparent ages range between 1855 and 1903 Ma, reflecting the variation in U and Pb contents in the magmatic system or the presence of mixed domains in the grains. Isotopic ratios of 13 zircons plot along a well-defined lead-loss line that intercepts the Concordia curve

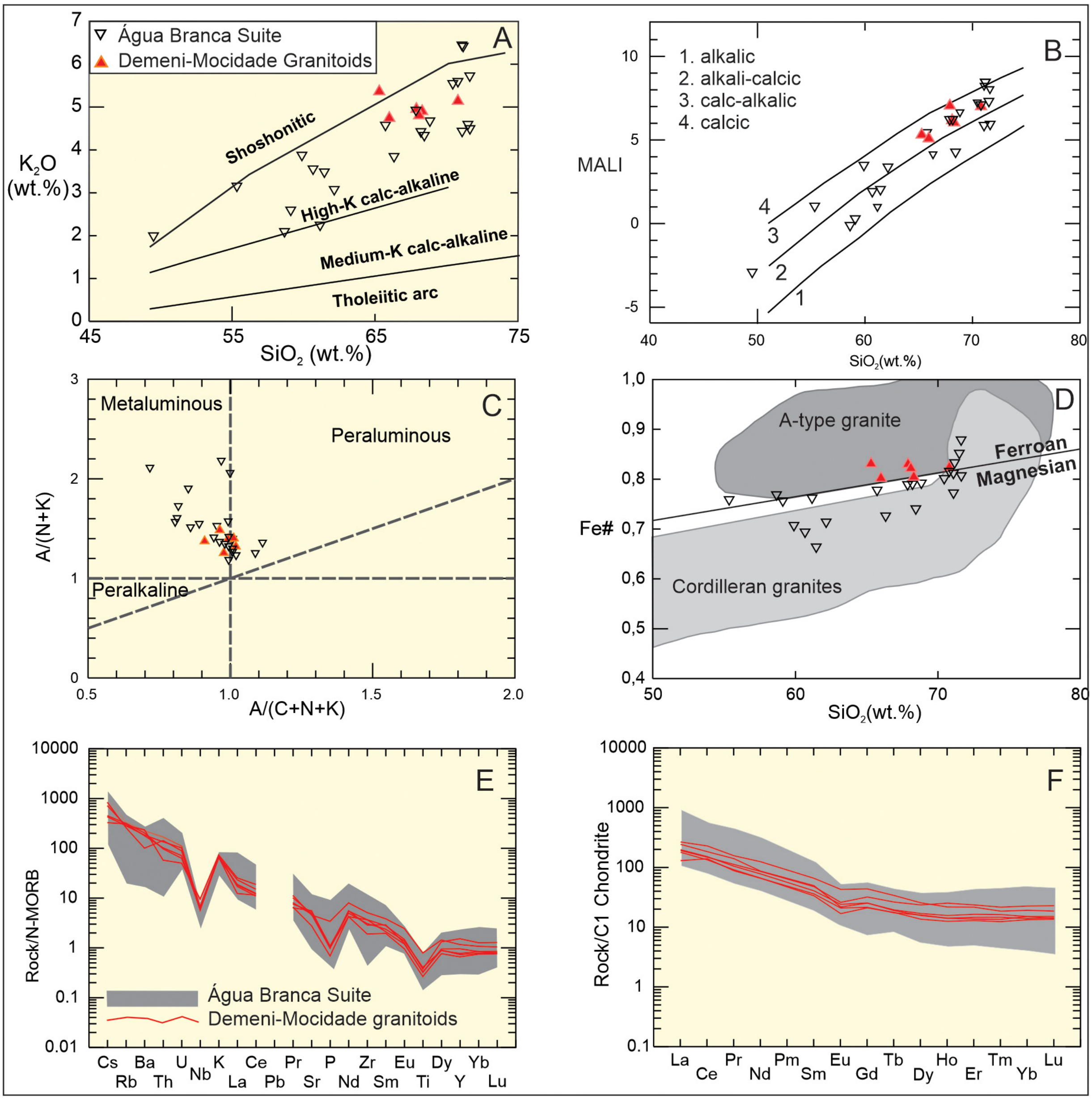

FIGURE 5. A) K_2O vs. SiO_2 discriminant diagram (Peccerillo and Taylor 1976) with high-K calc-alkaline pattern for the Água Branca Suite and Demêni-Mocidade granitoids; B) Modified alkali-calcic index diagram (MALI) vs. SiO_2 (Frost et al. 2001); C) Alumina saturation diagram (Maniar and Piccoli 1989) for classification of granitic rocks using Shand's Index (after Shand 1943). See limits for metaluminous, peraluminous and peralkaline fields. Al/Na+K and Al/Na+Ca+K are respectively molar ratios of Al_2O_3/Na_2O+K_2O and Al_2O_3/Na_2O+K_2O+CaO; D) Fe# vs. SiO_2 discriminant diagram for ferroan and magnesian types (Frost et al. 2001). Fe# means $Fe_2O_3t/(Fe_2O_3t + MgO)$ ratio; E) N-MORB-normalized (Sun and McDonough 1989) multi-element diagram; F) C1 chondrite–normalized rare-earth elements (REE) diagrams with normalization values from Sun and McDonough (1989). Whole-rock data of the Água Branca Suite (empty triangles) were published by Almeida (2006). Red triangles, this paper.

at 1880.5 ± 7.0 (± 9.1) Ma (Figure 7). This result is the best approximation of the crystallization age of this rock.

EC-97 Sample – Sizes of zircons selected from the samples range from 80 to 200µm. Many grains are elongate to short prismatic, not rarely with bipyramidal termination. Main internal structures, such as concentric zoning and mineral inclusions, are shown in detail in CL images, where they are highlighted by the distinct and contrasting brightness of each domain (grains 5.1, 6.1 and 7.1, Figure 6). Spot analyses yielded low-U (101-322 ppm) and Th (63-327) contents, resulting in Th/U ratios ≈ 0.55-1.35. Dating of selected zircons, with degrees of discordance ranging between -7 and 10% and $^{207}Pb/^{206}Pb$ apparent ages ranging from 1875 to 1901 Ma, indicate possible variation in U-Pb isotopic ratios during magmatic crystallization. Very importantly, the analysis of EC-97 (antecrystal spot 2.1) sample yielded a concordant $^{207}Pb/^{206}Pb$ age of 1901 Ma. Twelve isotopic analyses (autocrystals) plot on a relatively well-defined lead-loss line and yielded an upper

TABLE 4. U-Pb-SHRIMP II analytical data for zircons from the Demêni-Mocidade granitoids.

Spot Name	Ratios							^{206}Pb comm %	err Corr	Age (Ma)				Disc %	ppm		
	$^{207}Pb/^{235}U$	err %	$^{206}Pb/^{238}U$	err %	Corr	$^{207}Pb/^{206}Pb$	err %			$^{206}Pb/^{238}U$	1σ	$^{207}Pb/^{206}Pb$	1σ		U	Th	Th/U
EC-95																	
1.1	55.752	2.5	0.3523	2.3	0.937	0.1148	0.8	0.47	0.937	1945	39	1876	16	-4	209	141	0.70
2.1	50.374	2.4	0.3161	2.3	0.983	0.1156	0.4	0.04	0.983	1770	36	1889	8	7	219	189	0.89
3.1	52.272	2.4	0.3254	2.3	0.960	0.1165	0.7	0.14	0.960	1816	37	1903	12	5	127	74	0.60
4.1	55.730	2.5	0.3543	2.3	0.952	0.1141	0.7	0.38	0.952	1955	39	1865	14	-5	170	122	0.74
5.1	28.457	5.7	0.1819	2.4	0.415	0.1133	4.9	4.35	0.415	1077	23	1856	93	72	276	185	0.69
6.1	56.643	2.4	0.3571	2.3	0.975	0.1150	0.5	0.16	0.975	1968	40	1881	10	-4	170	117	0.71
7.1	41.022	4.3	0.2592	2.3	0.546	0.1147	3.3	2.97	0.546	1485	31	1877	64	26	354	186	0.54
8.1	48.046	2.5	0.3041	2.3	0.914	0.1146	1.0	0.69	0.914	1712	35	1874	19	9	334	248	0.77
9.1	55.508	2.5	0.3513	2.3	0.952	0.1146	0.7	0.25	0.952	1941	39	1873	14	-3	136	90	0.69
10.1	46.328	3.0	0.2962	2.4	0.777	0.1134	1.8	1.28	0.777	1672	35	1855	34	11	120	78	0.67
11.1	49.630	2.4	0.3119	2.4	0.979	0.1154	0.5	0.07	0.979	1750	36	1886	9	8	216	210	1.00
12.1	53.429	3.0	0.3366	2.3	0.793	0.1151	1.8	0.61	0.793	1870	38	1882	32	1	128	84	0.68
13.1	57.697	2.4	0.3677	2.3	0.962	0.1138	0.6	0.27	0.962	2019	40	1861	12	-8	139	103	0.77
14.1	53.720	2.5	0.3400	2.3	0.949	0.1146	0.7	0.45	0.949	1887	38	1874	14	-1	166	153	0.95
EC-97																	
1.1	55.767	2.4	0.3521	2.3	0.982	0.1149	0.5	0.02	0.982	1945	39	1878	8	-3	132	79	0.62
2.1	54.753	2.4	0.3412	2.3	0.961	0.1164	0.7	0.11	0.961	1893	38	1901	12	0	118	75	0.66
3.1	57.838	2.5	0.3663	2.4	0.956	0.1145	0.7	0.17	0.956	2012	41	1872	13	-7	101	63	0.65
4.1	47.439	2.4	0.3016	2.3	0.973	0.1141	0.6	0.04	0.973	1699	35	1865	10	10	171	93	0.56
5.1	51.239	2.5	0.3245	2.5	0.984	0.1145	0.4	0.07	0.984	1812	39	1872	8	3	251	327	1.35
6.1	54.229	2.4	0.3438	2.3	0.990	0.1144	0.3	0.03	0.990	1905	39	1871	6	-2	295	142	0.50
7.1	56.810	2.4	0.3582	2.4	0.979	0.1150	0.5	0.24	0.979	1974	40	1880	9	-5	322	334	1.07
8.1	48.017	2.4	0.3029	2.4	0.970	0.1150	0.6	0.08	0.970	1706	35	1880	11	10	122	68	0.58
9.1	50.481	2.4	0.3185	2.3	0.984	0.1150	0.4	0.01	0.984	1782	36	1879	8	5	223	132	0.61
10.1	50.562	2.4	0.3198	2.3	0.980	0.1147	0.5	0.08	0.980	1789	36	1875	8	5	208	221	1.10
11.1	54.557	2.4	0.3442	2.3	0.982	0.1149	0.4	0.04	0.982	1907	38	1879	8	-1	151	84	0.57
12.1	53.398	2.4	0.3332	2.3	0.976	0.1162	0.5	0.17	0.976	1854	38	1899	9	2	194	104	0.55
VC-37																	
1.1	144.991	2.9	0.6983	2.4	0.825	0.1509	1.5	0.38	0.825	3414	62	2353	28	-31	149	36	0.25
2.1	53.392	2.4	0.3415	2.3	0.955	0.1134	0.7	0.33	0.955	1894	38	1854	13	-2	145	79	0.56
3.1	49.997	2.6	0.3175	2.5	0.961	0.1142	0.7	0.24	0.961	1777	39	1868	13	5	171	140	0.84
4.1	52.572	2.4	0.3282	2.3	0.979	0.1162	0.5	0.08	0.979	1830	37	1898	9	4	209	161	0.79
5.1	62.554	3.2	0.4010	2.3	0.731	0.1132	2.1	1.10	0.731	2174	43	1850	40	-15	251	196	0.81
6.1	55.878	2.5	0.3511	2.3	0.940	0.1154	0.8	0.52	0.940	1940	39	1887	15	-3	185	112	0.62
7.1	59.462	2.4	0.3751	2.3	0.980	0.1150	0.5	0.21	0.980	2053	41	1879	9	-8	268	242	0.94
8.1	55.950	2.4	0.3567	2.3	0.965	0.1138	0.6	0.32	0.965	1966	39	1861	11	-5	185	163	0.91
9.1	52.574	2.5	0.3323	2.4	0.942	0.1148	0.8	0.55	0.942	1849	38	1876	15	1	273	188	0.71
10.1	52.758	2.5	0.3328	2.3	0.931	0.1150	0.9	0.54	0.931	1852	38	1880	16	2	153	120	0.81
11.1	51.984	2.3	0.3271	2.3	0.984	0.1153	0.4	0.19	0.984	1824	37	1884	8	3	376	406	1.11
12.1	50.702	2.5	0.3207	2.3	0.930	0.1147	0.9	0.55	0.930	1793	36	1875	16	5	632	774	1.27
NR-02																	
1.1	53.633	1.3	0.3362	1.2	0.863	0.1157	0.7	0.42	0.863	1868	19	1891	12	1	205	208	1.05
2.1	43.525	2.5	0.2736	1.8	0.729	0.1154	1.7	2.75	0.729	1559	25	1886	31	19	255	156	0.63
3.1	54.210	1.3	0.3441	1.1	0.877	0.1143	0.6	-0.05	0.877	1906	18	1868	11	-2	289	296	1.06
4.1	53.968	1.3	0.3388	1.1	0.885	0.1155	0.6	0.26	0.885	1881	18	1888	11	0	255	174	0.71
5.1	53.476	1.4	0.3380	1.2	0.832	0.1148	0.8	0.31	0.832	1877	19	1876	14	0	172	119	0.72
6.1	53.172	1.5	0.3397	1.2	0.804	0.1135	0.9	0.26	0.804	1885	19	1856	16	-2	175	112	0.66
7.1	51.309	1.3	0.3237	1.1	0.814	0.1149	0.8	0.74	0.814	1808	17	1879	14	4	412	559	1.40
8.1	55.036	1.3	0.3426	1.1	0.889	0.1165	0.6	0.17	0.889	1899	19	1903	11	0	217	172	0.82
NR-05																	
1.1	52.392	2.2	0.3309	1.3	0.578	0.1148	1.8	0.90	0.578	1843	20	1877	32	2	220	269	1.26
2.1	55.089	1.4	0.3479	1.3	0.915	0.1148	0.6	-0.27	0.915	1925	21	1877	10	-3	1275	1081	0.88
3.1	49.314	4.1	0.3197	1.5	0.368	0.1119	3.9	1.88	0.368	1788	24	1830	70	3	137	113	0.86
4.1	51.907	2.0	0.3274	1.2	0.588	0.1150	1.6	0.81	0.588	1826	19	1880	29	3	542	221	0.42
5.1	50.983	1.4	0.3220	1.2	0.852	0.1148	0.7	0.97	0.852	1799	18	1877	13	5	209	126	0.62
6.1	52.061	1.6	0.3344	1.1	0.711	0.1129	1.1	0.28	0.711	1860	18	1847	20	-1	233	222	0.98
7.1	54.681	1.4	0.3434	1.2	0.866	0.1155	0.7	-0.01	0.866	1903	20	1888	13	-1	136	109	0.83
8.1	53.902	1.7	0.3376	1.1	0.671	0.1158	1.3	0.39	0.671	1875	19	1893	23	1	216	98	0.47
NR-06																	
1.1	52.534	1.5	0.3302	1.2	0.807	0.1154	0.9	0.70	0.807	1840	19	1886	16	3	224	189	0.87
2.1	52.717	1.5	0.3308	1.2	0.788	0.1156	0.9	0.79	0.788	1842	19	1889	17	3	234	169	0.74
3.1	53.645	1.5	0.3349	1.2	0.782	0.1162	1.0	0.77	0.782	1862	19	1898	17	2	243	219	0.93
4.1	51.876	2.7	0.3282	1.2	0.451	0.1146	2.4	1.06	0.451	1830	19	1874	44	3	249	156	0.65
5.1	53.714	1.6	0.3432	1.1	0.709	0.1135	1.1	0.04	0.709	1902	18	1857	20	-3	256	157	0.63
6.1	54.900	1.2	0.3427	1.1	0.888	0.1162	0.6	0.19	0.888	1899	18	1899	10	0	330	260	0.81
7.1	53.339	1.5	0.3347	1.4	0.932	0.1156	0.5	0.45	0.932	1861	22	1889	10	2	352	298	0.87
8.1	54.270	1.2	0.3437	1.2	0.950	0.1145	0.4	-0.15	0.950	1904	19	1873	7	-2	499	308	0.64

intercept age of 1877.7 ± 4.9 (±7.6) Ma. Four out of these 12 analysis, with a higher agreement percentage, produced a model that yielded a concordant crystallization age of 1881.7 ± 4.8 Ma (Figure 7).

VC-37 Sample - The sample is formed by short prismatic zircon crystals, with subhedral to anhedral habit, and grain sizes ranging from 80 to 120 µm. Rounded grains are also present. In CL images, grains show concentric oscillatory zoning, and rarely small mineral inclusions, characterized by low contrast of shades of gray to black (grains 3.1 and 11.1, figure 6). In general, Th/U ratios range from 0.56 to 1.27, with concentrations of U = 145-632 and Th = 79-774. Eleven analyses, with $^{207}Pb/^{206}Pb$ apparent ages ranging from 1898 to 1850 Ma and degrees of discordance ranging from -15 to 5%, plot on a Pb-loss line that intercepts the Concordia at 1878.5 ± 6.9 (±9.0) Ma (Figure 7), which was interpreted as the best approximation of the crystallization age of the rock.

6. Discussion

The granitoids of the Água Branca Suite and those of the Demêni and Mocidade mountains share a common geochemical signature, which suggests a crystallization from primary magmas from chambers with identical character. In the petrographic study, a hiatal porphyritic texture was identified in some lithotypes containing phenocrysts with oscillatory zoning and resorbed rims, indicating that the crystallization occurred in a subvolcanic setting, under complex conditions.

The rocks are calc-alkaline, metaluminous and slightly peraluminous, and record clear Ti and Nb negative anomalies, suggesting formation from magmas derived from metamafic crustal sources (Castro et al. 2010), or from a metasomatized sub-lithospheric mantle (Aranovich et al. 2014, Castro 2019). In both cases, the magmatic processes may have produced residual material containing Fe-Ti-Nb-(Ta) oxides. The Eu/Eu* negative anomalies may have been formed by means of plagioclase fractioning during magma cooling within the crust or by the formation of residues containing plagioclase. LILE, LREE, U and Th enrichment is consistent for slightly oxidized I-type granites, formed from magmas which assimilated crustal elements during their ascension into the lithosphere. This hypothesis seems to be consistent with the presence of garnet in one of the study rocks.

The U-Pb SHRIMP ages obtained in zircon crystals of the granitic rocks are within the range 1882 and 1877 Ma, which probably corresponds to the main period of crystallization of the crustal segment Demêni-Mocidade, with a duration of about 5 Ma. Concordant $^{207}Pb/^{206}Pb$ apparent ages ranging from 1903 to 1899 Ma suggest slightly older magmatism than the one bracketed by the intercept ages, and it may be interpreted

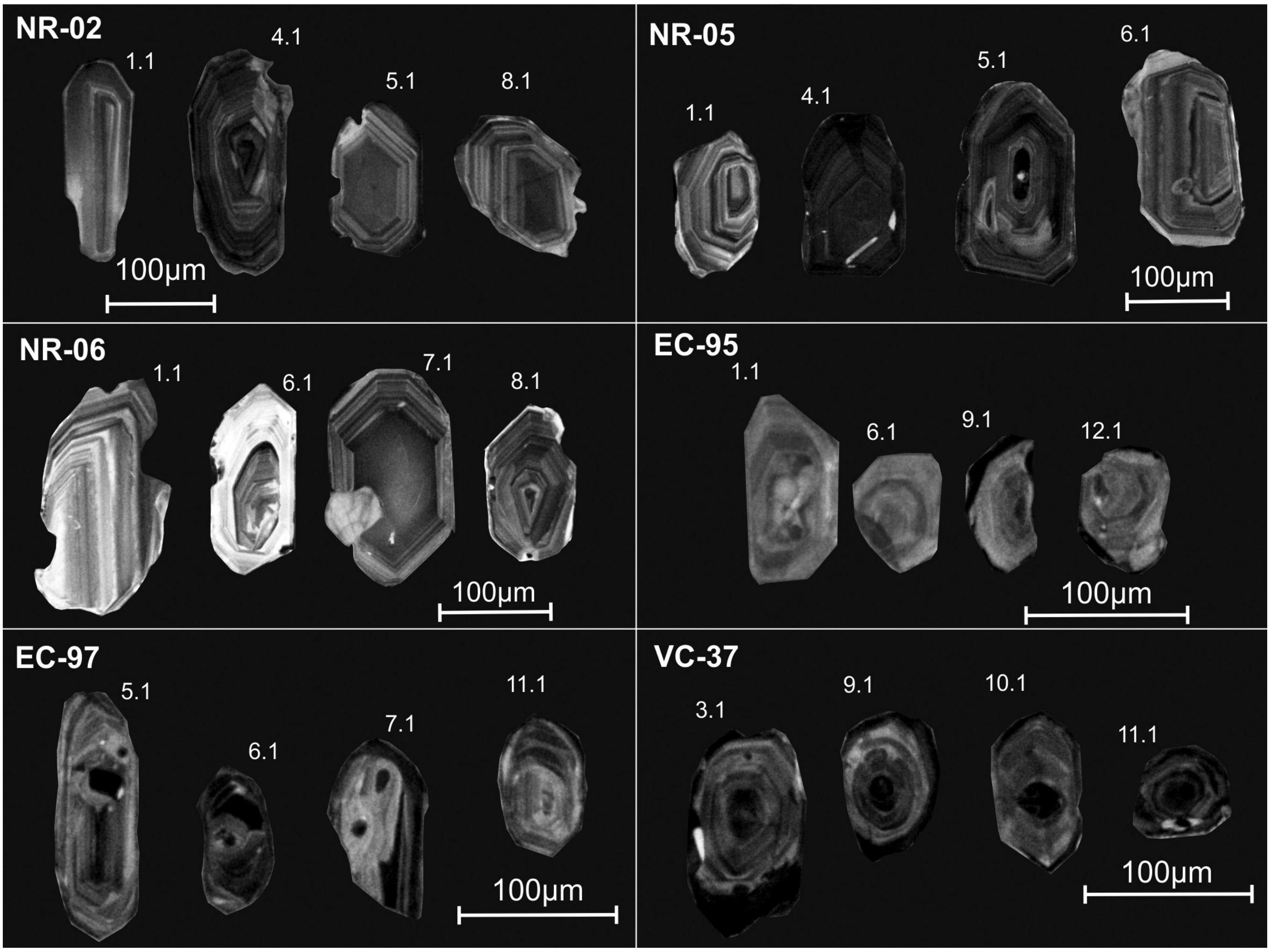

FIGURE 6. CL images of selected zircon grains for SHRIMP dating.

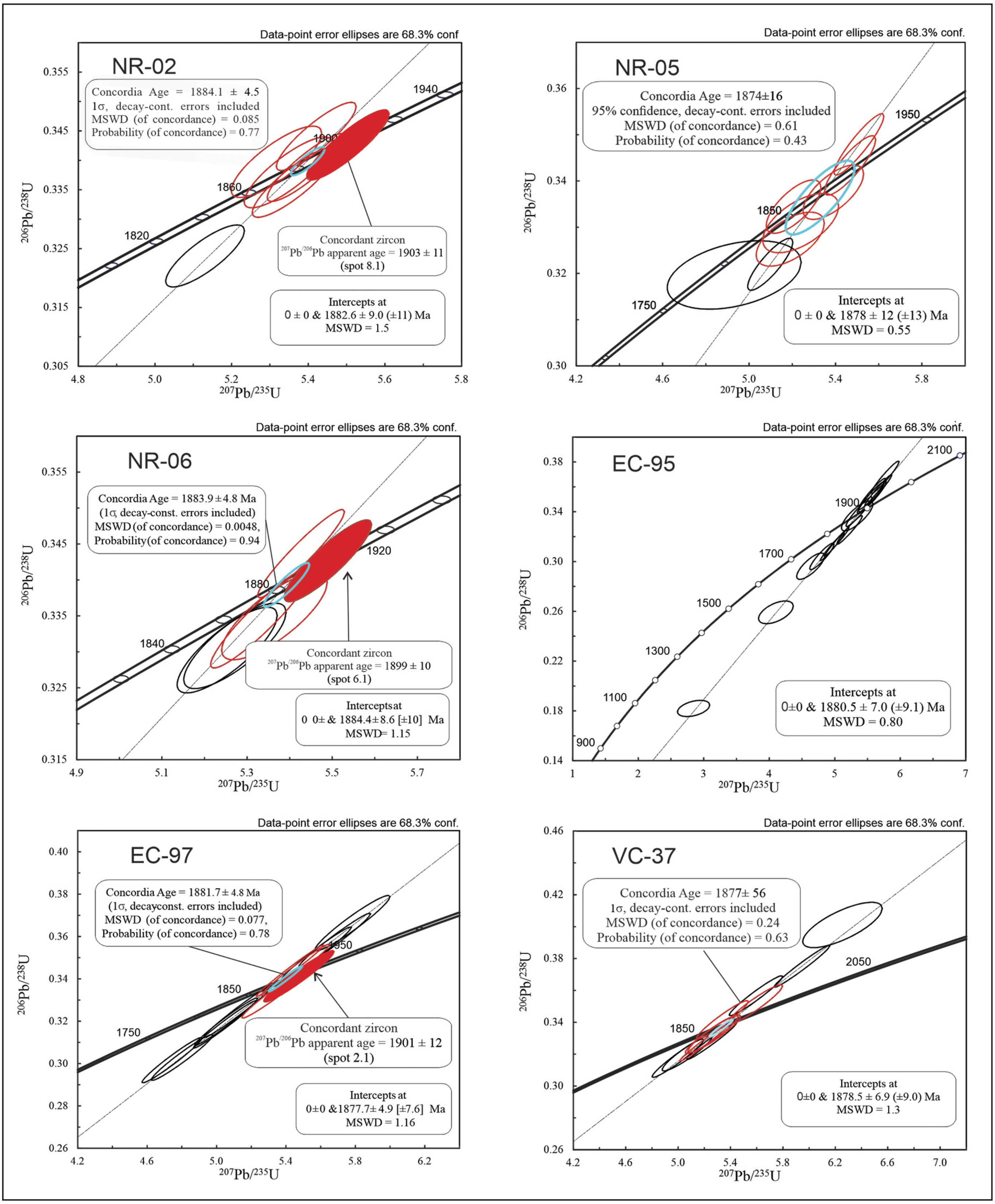

FIGURE 7. Concordia diagrams for rocks from the Demêni-Mocidade Domain.

as the formation of the first magmatic products. Pb/Pb zircon evaporation ages of 1.90 Ga were found for the Água Branca Suite, in the southeast of Roraima (Almeida 2006).

The T_{DM} model ages of the Água Branca Suite in the southern part of the Guiana Shield are predominantly Siderian and Rhyacian, and negative eNd values suggest a derivation from either crustal or juvenile sources (Almeida 2006). Nd Archean model ages were not encountered (Vasquez and Rosa-Costa 2008, Barreto et al. 2013, Leal et al. 2018). However, Semblano et al. (2016), working with similar calc-alkaline granites of the Iriri-Xingu Domain of the Central Brazil Shield, indicated that some Archean crustal material may have been mixed with juvenile Paleoproterozoic material. Likewise, the Siderian Nd model ages found by Almeida (2006) may also be a result of mixing sources of Archean and Paleoproterozoic ages.

Shallow magmatic processes - in which volcanic and plutonic rocks are found closely associated - have been envisaged. Pearce et al. (1984), by means of geochemical studies, suggested that A-type alkalic granites are linked to anorogenic/intraplate environments, while Sylvester (1989), Bonin (1990) and others argued that alkali granites may also be formed during post-orogenic pulses. They could follow a subduction period, as the end-product of a magmatic cycle dominated by a calc-alkalic series.

The calc-alkalic granitic types which occur within the Uatumã SLIP are considered by several authors to be formed as magmatic arcs within orogenic environments (Santos 2003, Tassinari and Macambira 2004, Cordani and Teixeira 2007, Valério et al. 2012 and references therein) and shall be distinguished from anorogenic types associated to intraplate episodes. However, several other authors (Almeida 2006, Vasquez and Rosa-Costa 2008, Klein et al. 2012, Fraga et al. 2017, Roverato et al. 2019) argued that calc-alkaline magmatism may be generated in processes not associated with subduction, but linked with intracontinental environments, with more stable tectonic conditions, where A-type granites can also be formed.

Therefore, different interpretations for the tectonic environment of the extremely large Uatumã SLIP were presented and remain under debate. For example, Almeida (2006) argues for a process of magmatic underplating, with different types of sources, such as crustal fusion of ancient material, or juvenile mantle addition.

The Aracá Table, in the Corrupira mountain range, can express geodynamic processes generated in an intracontinental rift environment subsequent to that of the post-orogenic Uatumã SLIP. According to Larizzatti and Giovannini (1994), the Aracá Table includes sedimentary rocks with different degrees of deformation with mylonitic textures developed in restricted shear zones which, in turn, are linked to some deformational episodes. In this way, the Aracá sedimentary set may not be entirely metamorphic, as conceived by Luzardo (2002).

Detrital zircon grains from the Aracá Table indicated source ages associated with the Uatumã SLIP and to the Rio Urubu Belt, thus generating some doubt about the age of the basement, whose 1.79 Ga age is possibly situated more to the west and outside of the main area of the sedimentary cover.

7. Final remarks

The DMD considered in this study, in the central part of the Guiana Shield, makes up the northern portion of the Ventuari-Tapajós tectonic province. The association between plutonic and subvolcanic rocks in the same suite shows variations in the crustal development of several magmatic chambers and conduits, matching similar geological situations found in the Uatumã SLIP in many other different places. Although in a small number, the six samples of the granitoids analyzed in this study could offer petrographic, geochemical, and geochronological characters that enabled such correlation.

The coexistence between I- and A-type granitoids, with ages within the range 1.88-1.87 Ga, stimulates the following discussion: a) if the calc-alkaline magmatism is associated with late (post-collisional) processes related to subduction; b) if they were formed in an intracontinental setting under more stable (post-orogenic to intraplate) tectonic crustal conditions and, c) if they were predominantly formed in intraplate settings by A-type and alkaline magmatism.

Acknowledgements

The authors would like to thank professor Mario Cohn-Haft from the National Institute of Amazonian Research – INPA for coordinating the teams and fieldworks in the Mocidade Mountain; the GRIFA Filmes company for offering financial support and endorsing the research; the biologist Erica Fugisaki from the Chico Mendes Institute for Biodiversity Conservation – ICMBio for the management of the Serra da Mocidade National Park and for permission to collect rocks; and the Amazon Military Command – CMA for supporting jungle operations. We are also thankful to the State of São Paulo Research Foundation – FAPESP for financial support under grant number 12754-0 awarded to Umberto Cordani (USP). We are also grateful to the anonymous reviewer and Dr. Moacir Macambira (UFPA) for their valuable suggests and comments and to the Editor-In-Chief, whose commenst and remarks helped us to improve the manuscript.

References

Almeida M.E. 2006. Evolução geológica da porção centro-sul do Escudo das Guianas com base no estudo geoquímico, geocronológico e isotópico dos granitóides Paleoproterozóicos do sudeste de Roraima, Brasil. PhD Thesis, Centro de Geociências da Universidade Federal do Pará, Belém, 227 p. Available on line at: http://rigeo.cprm.gov.br/jspui/handle/doc/172 / (accessed on 10 June 2020).

Almeida M.E., Macambira M.J.B. 2007. Geology and petrography of paleoproterozoic granitoid from Uatumã-Anauá Domain, central region of Guyana Shield, southeastern Roraima, Brazil. Revista Brasileira de Geociências, 37, 2, 237-256. Available on line at: http://ppegeo.igc.usp.br/index.php/rbg/article/view/9272/8751 / (accessed on 10 June 2020).

Almeida M.E., Macambira M.J.B., Santos, J.O.S., Nascimento R.S.C.do, Paquette J-L. 2013. Evolução crustal do noroeste do Cráton Amazônico (Amazonas, Brasil) baseada em dados de campo, geoquímicos e geocronológicos. In: Simpósio de Geologia da Amazônia, 13, 4 p.

Aranovich L.Y., Makhluf A.R., Manning C.E., Newton R.C. 2014. Dehydration melting and the relationship between granites and granulites. Precambrian Research, 253, 26-37. http://dx.doi.org/10.1016/j.precamres.2014.07.004

Barreto C.J.S., Lafon J.M., Costa L.T.R., Lima E.F. 2013. Vulcanismo félsico Paleoproterozoico do Grupo Iricoumé, Domínio Erepecuru-Trombetas, Província Amazônia Central: dados de campo, caracterização petrográfica e geocronologia Pb-Pb em zircão. Geologia USP. Série Científica 13, 1, 47-72. https://doi.org/10.5327/Z1519-874X2013000100004

Berrangé J.P. 1977. The geology of Southern Guyana, South America. Institute of Geological Sciences. Overseas Memoir, 4. London, H.M. Stationery Off.,112 p.

Black L.P., Kamo S.L., Allen C.M., Aleinikoff J.N., Davis D.W., Korsch R. J., Foudoulis C. 2003. TEMORA 1: a new zircon standard for Phanerozoic U–Pb geochronology. Chemical Geology, 200, 1-2, 155-170. https://doi.org/10.1016/S0009-2541(03)00165-7

Bonin B. 1990. From orogenic to anorogenic settings: evolution of graniloids suites after a major orogenesis. Geological Journal, 25, 1-11. https://doi.org/10.1002/gj.3350250309

Castro A. 2019. The dual origin of I-type granites: The contribution from laboratory experiments. In: Janoušek V., Bonin B., Collins W.J., Farina F., Bowden P. (ed.). Post-Archean Granitic Rocks: petrogenetic processes and tectonic environments. Geological Society, London, Special Publications 491, 101-145. Available on line at: https://doi.org/10.1144/SP491-2018-110

Castro A., Gerya T., García-Casco A., Fernández C., Diáz-Alvarado J., Moreno-Ventas I., Löw I. 2010. Melting Relations of MORB-Sediment Mélanges in Underplated Mantle Wedge Plumes; Implications for the Origin of Cordilleran-type Batholiths. Journal of Petrology, 51, 6, 1267-1295. https://doi.org/10.1093/petrology/egq019

Chiarini M.F.N., Rocha L.G.M., Oliveira A.C.S. 2018. Carta geofísica-geológica: folha Rio Padauari, NA.20-Y-D. Manaus, CPRM, 2018. 1 mapa, Escala 1:250.000. Available on line at: http://rigeo.cprm.gov.br/jspui/handle/doc/20275 / (accessed on 01 November 2020).

Cordani U.G., Teixeira W. 2007. Proterozoic Accretionary Belts in the Amazonian Craton. Geological Society of America Memoir, 200, 297-319. https://doi.org/10.1130/2007.1200(14)

Cordani U.G., Fraga L.M., Reis N.J., Tassinari C.C.G., Brito-Neves B.B. 2010. On the origin and tectonic significance of the intra-plate events of Grenvillian-type in South America: A discussion. Journal of South American Earth Sciences, 29, 143-159. https://doi.org/10.1016/j.jsames.2009.07.002

Correa R.T. 2019. Mapa magnetométrico do Brasil. Brasília, Serviço Geológico do Brasil – CPRM, 1 mapa, Escala 1:5.500.000. Available on line at: http://rigeo.cprm.gov.br/jspui/handle/doc/21299 / (accessed on 01 November 2020).

Costi H.T., Santiago A.F., Pinheiro S.S. 1984. Projeto Uatumã-Jatapu / Jatapu: relatório final. Manaus, CPRM, 133 p. Available on line at: http://rigeo.cprm.gov.br/jspui/handle/doc/3523

Costi H.T., Valério C.S., Alves M.A.S., Souza V.S. 2009. Overview of the geology of Southernmost Guyana Shield, north of Presidente Figueiredo district, NE Amazonas. In: Simpósio de Geologia da Amazônia, 11, 4 p.

Ferron J.M.T.M., Bastos Neto A.C., Lima F., Nardi L.V.S., Costi H.T., Pierosan R., Prado M. 2010. Petrology, geochemistry, and geochronology of Paleoproterozoic volcanic and granitic rocks (1.89–1.88 Ga) of the Pitinga Province, Amazonian Craton, Brazil. Journal of South American Earth Sciences, 29, 483-497. https://doi.org/10.1016/j.jsames.2009.05.001

Fraga L.M., Reis N.J. 2002. The Calc-Alkaline Volcano-Plutonism in the Northern Roraima State, Guiana Shield: implications for the Uatumã Event Concept and Geotectonic Significance. In: Simpósio de Vulcanismo e Ambientes Associados, 2, p. 24.

Fraga L.M., Vasquez M.L., Almeida M.E., Dreher A.M., Reis N.J. 2017. A Influência da Orogenia Eo-Orosiriana na formação da SLIP Uatumã, parte central do Cráton Amazônico. In: Simpósio de Geologia da Amazônia, 15, 405-408.

Frost B.R., Barnes C. G., Collins W. J., Arculus R. J., Ellis D. J., Frost C. D. 2001. A geochemical classification for granitic rocks. Journal of Petrology 42, 11, 2033-2048. https://doi.org/10.1093/petrology/42.11.2033

Gaudette H.E., Olszewski Jr. W.J. 1985. Geochronology of the basement rocks, Amazonas Territory, Venezuela and the tectonic evolution of the western Guiana Shield. Geologie en Mijnbouw 64, 131-143.

Klein E.L., Almeida M.E., Rosa-Costa L.T. 2012. The 1.89-1.87 Ga Uatumã Silicic Large Igneous Province, northern South America. November 2012 LIP of the Month. Available on line at: http://www.largeigneousprovinces.org/12nov / (accessed on 01 November 2020).

Larizzatti J.H., Giovannini C.A. 1994. Contribuição à geologia da Serra Aracá, Amazonas. In: Simpósio de Geologia da Amazônia, 4, 15-17.

Leal R.E., Lafon J.M., Rosa-Costa L.T., Dantas E.L. 2018. Orosirian magmatic episodes in the Erepecuru-Trombetas Domain (southeastern Guyana shield): implications for the crustal evolution of the Amazonian Craton. Journal of South American Earth Sciences, 85, 278-297. https://doi.org/10.1016/j.jsames.2018.04.011

Ludwig K.R. 2009a. SQUID 2: A User's Manual, rev. 12 Apr, 2009. Berkeley, Berkeley Geochronology Center, Special Publication 5, 110 p.

Ludwig K.R. 2009b. User's Manual for Isoplot 3.70. Special Publication 4. Berkeley, Berkeley Geochronology Center, 76 p.

Luzardo R. 2002. Metamorfismo da Serra Aracá, Amazonas. In: Congresso Brasileiro de Geologia, 41, p. 316.

Macambira M.J.B., Almeida M.E., Santos L.S. 2002. Idade de Zircão de vulcânicas do sudeste de Roraima: contribuição para a redefinição do Supergrupo Uatumã. In: Simpósio de Vulcanismo e Ambientes Associados, 2, 4 p.

Maniar P.D., Piccoli P.M. 1989. Tectonic Discrimination of Granitoids. Geological Society of America Bulletin 101, 5, 635-643. https://doi.org/10.1130/0016-7606(1989)101<0635:TDOG>2.3.CO;2

Marques S.N.S., Souza V.S., Dantas E.L., Valério C.S., Nascimento R.S.C. 2014. Contributions to the petrography, geochemistry and geochronology (U-Pb and Sm-Nd) of the Paleoproterozoic effusive rocks from Iricoumé Group, Amazonian Craton, Brazil. Brazilian Journal of Geology, 44, 121-138. DOI:10.5327/Z2317-4889201400010010

Miller J.S., Matzel J.E.P., Miller C.F., Burgess S.D., Miller R.B. 2007. Zircon growth and recycling during the assembly of large, composite arc plutons. Journal of Volcanology and Geothermal Research, 167, 282-299. https://doi.org/10.1016/j.jvolgeores.2007.04.019

Oliveira A.C.S. 2018. Folha NA.20-Z-A Rio Catrimani: carta geofísica-geológica. Manaus, CPRM, 2018. 1 mapa, color. Escala 1:250.000. Available on line at: http://rigeo.cprm.gov.br/jspui/handle/doc/17805 / (accessed on 01 November 2020).

Oliveira M.J.R., Almeida M.E., Luzardo R., Faria M.S.G. 1996. Litogeoquímica da Suíte Intrusiva Água Branca - SE de Roraima. In: Congresso Brasileiro de Geologia, 39, v. 2.

Pearce J.A., Harris N.B.W., Tindle A.G. 1984. Trace element discrimination diagrams for the tectonic interpretation of granitic rocks. Journal of Petrology, 25, 4, 956-983. https://doi.org/10.1093/petrology/25.4.956

Peccerillo A., Taylor S.R. 1976. Geochemistry of Eocene Calc-Alkaline Volcanic Rocks from the Kastamonu Area, Northern Turkey. Contributions to Mineralogy and Petrology 58, 1, 63-81. https://doi.org/10.1007/BF00384745

Pinheiro S.S., Nunes A.C.B., Costi H.T.,Yamaguti H.S., Faraco M.T.L., Reis N.J., Menezes R.G. de, Riker S.R.L., Wildner W. 1981. Projeto Catrimâni-Uraricoera: relatório de progresso. Manaus, DNPM, CPRM, 2 v. Available on line at: http://rigeo.cprm.gov.br/jspui/handle/doc/7291 / (accessed on 01 November 2020).

Reis N.J., Faria M.S.G., Almeida M.E., Oliveira M.A. 2004. Folhas NA.20-Boa Vista e NB.20-Roraima. Brasília, CPRM. Escala 1:1.000.000. Programa Geologia do Brasil. http://rigeo.cprm.gov.br/jspui/handle/doc/4963 / (accessed on 01 November 2020).

Reis N.J., Almeida M.E., Riker S.R.L., Ferreira A.L. 2006. Geologia e recursos minerais do estado do Amazonas. Rio de janeiro, CPRM, CIAMA, 2006. Programa Geologia do Brasil. http://rigeo.cprm.gov.br/jspui/handle/doc/2967

Rocha L.G.M., Oliveira A.C.S., Chiarini M.F.N. 2018. Carta geofísica-geológica: folha Serra Gurupira, NA.20-Y-B. Manaus: CPRM, 2018. 1 mapa, color. Escala 1:250.000. Programa Geologia do Brasil. Available on line at: http://rigeo.cprm.gov.br/jspui/handle/doc/20277

Rossetti D.F., Molina E.C., Cremon E.H. 2016. Genesis of the largest Amazonian wetland in northern Brazil inferred by morphology and gravity anomalies. Journal of South America Earth Sciences 69, 1-10. https://doi.org/10.1016/j.jsames.2016.03.006

Roverato M., Giordano D., Giovanardi T., Juliani C., Polo L. 2019. The 2.0-1.88 Ga Paleoproterozoic evolution of the southern Amazonian Craton (Brazil): an interpretation inferred by lithofaciological, geochemical and geochronological data. Gondwana Research, 70, 1-24. https://doi.org/10.1016/j.gr.2018.12.005

Santos J.O.S. 2003. Geotectônica dos Escudos das Guianas e Brasil Central. In: Bizzi L.A., Schobbenhaus C., Vidotti R.M., Gonçalves J.H. (ed.). Geologia, tectônica e recursos minerais do Brasil: texto, mapas e SIG. Brasilia, CPRM. Cap. 4, 169-226. http://rigeo.cprm.gov.br/jspui/handle/doc/5006

Santos J.O.S., Bremen O.B.V., Groves D.I., Hartmann L.A., Almeida M.E., McNaughton N.J., Fletcher I.R. 2004. Timing and evolution of multiple Paleoproterozoic magmatic arcs in the Tapajós Domain, Amazon Craton: constraints from SHRIMP and TIMS zircon, baddeleyite and titanite U-Pb Geochronology. Precambrian Research, 131, 73-109. https://doi.org/10.1016/j.precamres.2004.01.002

Santos J.O.S., Faria M.S.G., Hartmann L.A., McNaughton N.J. 2002. Significant Presence of the Tapajós – Parima Orogenic Belt in the

Roraima Region, Amazon Craton based on SHRIMP U-Pb zircon Geochronology. In: Congresso Brasileiro de Geologia, 41, p. 336.

Santos J.O.S., Hartmann L.A., Faria M.S.G. de, Riker S.R.L., Souza M.M. de, Almeida M.E., McNaughton N.J. 2006. A Compartimentação do Cráton Amazonas em Províncias: Avanços ocorridos no período 2000-2006. In: Simpósio de Geologia da Amazônia, 9, 4 p.

Santos J.O.S., Pinto V., McNaughton N.J., Almeida M.E. 2011. Diversos episódios de magmatismo charnockítico no centro-norte do Cráton Amazonas: Província Tapajós – Parima e Rio Negro. In: Simpósio de Geologia da Amazônia, 11, 4 p.

Sato K., Tassinari C.C.G., Basei M.A.S., Siga Jr., O., Onoe A.T., Souza M.D. 2014. Sensitive High Resolution Ion Microprobe (SHRIMP IIe/MC) of the Institute of Geosciences of the University of São Paulo, Brazil: analytical method and first results. Geologia USP, Série Científica, 14, 3, 3-18. https://doi.org/10.5327/Z1519-874X201400030001

Semblano F.R.D., Pereira N.C.S., Vasquez M.L., Macambira M.J.B. 2016. Novos dados geológicos e isotópicos para o Domínio Iriri-Xingu, Província Amazônia Central; implicações para a idade do Grupo Iriri. Revista do Instituto de Geociências - USP, Série Científica, 16, 3, 19-38. https://doi.org/10.11606/issn.2316-9095.v16i3p19-38

Shand S.J. 1943. Eruptive Rocks. Their Genesis Composition. Classification, and Their Relation to Ore-Deposits with a Chapter on Meteorite. John Wiley & Sons, New York.

Streckeisen A. 1976. To each plutonic rock its proper name. Earth-Science Reviews, 12, 1-33. https://doi.org/10.1016/0012-8252(76)90052-0

Sun S.–S., McDonough W.F. 1989. Chemical and isotopic systematics of oceanic basalts: implications for mantle compostion and processes. In: Saunders, A.D., Norry, M.J. (ed.). Magmatism in the Ocean Basins. Geological Society, London, Special Publication, 42, 313-345. https://doi.org/10.1144/GSL.SP.1989.042.01.19

Sylvester P.J. 1989. Post-collisional alkaline granites. Journal of Geology, 97, 261-280. https://www.jstor.org/stable/30068745

Tassinari C.G.C., Macambira M.J.B. 2004. A evolução tectônica do Cráton Amazônico. In: Mantesso-Neto V., Bartorelli A., Carneiro C.D.R., Brito Nevez B.B.B. (ed). Geologia do Continente Sul-Americano: evolução da obra de Fernando Flávio de Almeida. São Paulo, Beca. Cap. XXVIII, 471-486.

Valério C.S., Macambira M.J.B., Souza V.S. 2012. Field and petrographic data of 1.90-1.88 Ga I- and A-type granitoids from the central Amazonian Craton, NE Amazonas State, Brazil. Revista Brasileira de Geociências, 42, 4, 690-712. DOI: 10.5327/Z0375-75362012000400004

Vasquez M.L., Cordani U.G., Sato K., Barbosa J.P.O., Faraco M.T.L., Maurer V.C. 2019. U-Pb SHRIMP dating of basement rocks of the Iriri-Xingu domain, Central Amazonian province, Amazonian craton, Brazil. Brazilian Journal of Geology, 49, 3. https://doi.org/10.1590/2317-4889201920190067

Vasquez M.L., Rosa-Costa L.T. (org.). 2008. Geologia e recursos minerais do estado do Pará: texto explicativo. Belém, CPRM, 328 p. Escala 1:1.000.000. Programa Geologia do Brasil - PGB. Available on line at: http://rigeo.cprm.gov.br/jspui/handle/doc/10443/ (accessed on 20 January 2021)

Williams I.S. 1998. U-Th-Pb geochronology by ion microprobe. In: McKibben M.A., Shanks I., Ridley W.C.P., Ridley W.I. (ed.). Application of Microanalytical Techniques to Understanding Mineralizing Process. El Paso, Society of Economic Geologists, Reviews in Economic Geology, 7, 1-35. https://doi.org/10.5382/Rev.07

Wynn J.C., Olmore S.D., Mendoza V., García A., Martínez M., Schruben P. 1994. Geological Map of the Venezuela Part of the Río Mavaca 2ox3o Quadrangle, Amazonas Federal Territory, Venezuela. USGS/CVG. https://doi.org/10.3133/mf2241